Quantum-Enhanced Dimensionality Reduction: Bridging Classical and Quantum Machine Learning

Asif Akhtab Ronggon[a,f], Tuhin Hossain[b,f], Khairul Alam[c,f], Syed Emad Uddin Shubha[d], Mahdy Rahman Chowdhury[e,*]

[a]*Department of Electrical and Electronic Engineering, Bangladesh University of Engineering and Technology, Dhaka, Bangladesh*
[b]*Department of Computer Science and Engineering, Jahangirnagar University, Savar, Bangladesh*
[c]*Department of Electrical and Electronics Engineering, Dhaka University of Engineering Technology, Gazipur, Bangladesh*
[d]*Department of Computer Science, Louisiana State University, Baton Rouge, USA*
[e]*Department of Electrical and Computer Engineering, North South University, Bashundhara R/A, Dhaka, Bangladesh*
[f]*Mahdy Research Academy*

Abstract

The proliferation of high-dimensional datasets in artificial intelligence(AI), healthcare, and finance has altered data-driven decision-making, but there are also significant computational and analytical issues. Recently, machine learning(ML) and quantum computing(QC) have advanced. Classical data processing and ML techniques used in QC have led to quantum machine learning(QML). As QC and QML boost processing speed and capacity due to their parallelism, they have garnered attention in various fields. Traditional dimensionality reduction(DR) methods like principal component analysis (PCA) minimize redundancy and increase interpretability, but massive data processing overhead restricts scalability. As a paradigm change based on quantum mechanical ideas like entanglement and superposition, this research looks at how QC could address these challenges. To improve DR and ML workflows, a quantum-inspired technique combines classical PCA, Kernel-PCA(KPCA), quantum principal component analysis(QPCA), and quantum variational autoencoders(QVAE). These approaches are tested on three individual datasets. First, we calculated the chi-square value to select four significant features for the target variable in all datasets. Then we employed classical and quantum models like support vector machine(SVM) and Quantum Neural Network(QNN). Although quantum approaches reduce dimensionality better than classical ML techniques, traditional ML models outperform quantum classifiers, emphasizing scalability and optimization concerns in QML models. When QPCA reduced the dataset dimensionality in the Breast Cancer dataset, the SVM model achieved 95% accuracy. In the Banknote and DARWIN datasets, SVM models performed best for QPCA at 98% and 80%. It demonstrated that classical-quantum hybrid architectures may address multidimensional challenges and utilize quantum systems in ML pipelines.

Keywords: Dimensionality Reduction(DR), Principal Component Analysis(PCA), Kernel-PCA(KPCA), Quantum Principal Component Analysis (QPCA), Quantum Variational Autoencoders (QVAE), Classical Machine Learning Quantum Machine Learning (QML), Hybrid Classical-Quantum Systems, High-Dimensional Data, Quantum Neural Networks (QNNs)

1. Introduction

The exponential growth of high-dimensional datasets in contemporary science and industry has fundamentally reshaped domains such as finance, healthcare, physics, and AI [1]. These datasets have the potential to unlock transformative insights, but they simultaneously pose substantial challenges. High-dimensional data are often characterized by redundancy, noise, and computational inefficiencies, which can deteriorate the achievement of ML models. DR approaches are therefore indispensable for distilling complicated datasets into their most informative features, enhancing both the interpretability and performance of the model. ML models have been taught on transformed datasets to assess

*Corresponding author
Email addresses: asifaftab172@gmail.com (Asif Akhtab Ronggon), tuhin97.hossain@gmail.com (Tuhin Hossain), khairulalamdidar@gmail.com (Khairul Alam), sshubh1@lsu.edu (Syed Emad Uddin Shubha), mahdy.chowdhury@northsouth.edu (Mahdy Rahman Chowdhury)

the following effects of the implemented methods for reducing dimensionality. Traditional approaches to DR, such as PCA, KPCA, have been extensively employed due to their conceptual simplicity and effectiveness. PCA reduces data dimensionality by identifying directions of maximum variance, thereby mitigating redundancy and simplifying analysis. Although PCA and similar methods have numerous uses in traditional ML, they always encounter problems when dealing with large datasets. The application of QC as a novel paradigm for ML and data analysis has sparked intrigue due to its shortcomings, such as enormous computation needs and long calculation durations [2]. For jobs that classical computers couldn't do, quantum computers use quantum mechanical ideas like entanglement, quantum parallelism, and superposition. Quantum computers are able to efficiently handle high-dimensional information because they operate within Hilbert spaces, which are exponentially bigger. The creation of quantum algorithms for DR like QPCA and QVAE was driven by the hope of achieving such capabilities. The use of quantum linear algebra subroutines in QPCA allows for principal component calculations to occur at an exponentially faster rate than in traditional PCA [3, 4]. On the other hand, QVAE expands these capabilities for generative modeling by providing effective techniques for encoding and decoding high-dimensional data.

Using both conventional and quantum approaches to DR, this paper presents a holistic methodology and analyzes their effects on ML procedures. The suggested methodology begins with normalization and other preprocessing processes to handle missing information, then moves on to feature selection using statistical methods like the chi-square test. Four methods follow dimensionality reduction: PCA and KPCA, a control method with a long history in the field, and QPCA and QVAE, both of which are influenced by quantum mechanics. The efficacy, scalability, and computing efficiency of classical and quantum approaches to reducing large-scale data may be thoroughly assessed via the integrated framework [5]. The paper's key contributions are as follows:

- Propose a hybrid model that integrates traditional and quantum computing methodologies to investigate the potential advantages of quantum techniques in high-dimensional ML classification tasks.
- Evaluate the effectiveness of QPCA and QVAE in comparison to classical PCA and KPCA in terms of their influence on classification performance.
- Conduct an extensive analysis between QNN and classical SVM, demonstrating that classical models constantly outperform QNNs across a variety of datasets, particularly when combined with QPCA.

The subsequent sections are structured as follows. Section 2 provides a review of relevant literature. Section 3 provides a comprehensive description of the background material utilized in this research work, which includes the two primary components, classical and quantum ML, along with the methodology applied. This section emphasizes the data set, the models under investigation, and the proposed quantum-inspired classical model. Section 4 details the experimental investigation, the findings, and the model's interpretation. Section 5 presents the conclusions and outlines future work.

2. Literature Review

QML has seen remarkable advancements, demonstrating its potential across diverse fields while addressing inherent challenges. Several researchers have proposed quantum algorithms specifically designed for data representation and analysis for ML applications. The paper introduces quantum algorithms leveraging Singular Value Decomposition (SVD) for data representation and analysis, focusing on PCA, Correspondence Analysis, and Latent Semantic Analysis. By attaining competitive classification performance with efficient runtime and low errors, it exhibits practical applications and offers theoretical insights into runtime and error boundaries [6]. To achieve exponential speedups over traditional PCA, an accurate QPCA technique was introduced that utilized quantum singular value thresholding (QSVT). By taking use of quantum parallelism, this innovation was able to handle high-dimensional data with a temporal complexity that was lowered from $O(N^3)$ to $O(N \,\mathrm{poly}(\log N))$. The method's verification on IBM Quantum Experience is a major step towards using quantum algorithms in real-world ML problems [7].

A low-complexity QPCA strategy emerged that reduced the number of phase estimations needed to simplify quantum circuits. Considering the findings of this investigation, it is possible to use QPCA on noisy intermediate-scale quantum (NISQ) devices, which might reduce runtime by 60% compared to traditional quantum approaches [8]. Another researcher used a combination of traditional and quantum methods to conduct QPCA on the Yale Face Dataset, with an emphasis on eigenface extraction for face identification. The study found that QPCA can handle high-dimensional data when combined with future advancements in quantum RAM, even though there was no significant quantum speedup due to current hardware limitations [9].

Quantum covariance matrices that use amplitude encoding will have been the subject of much research. Encoding algorithms tailored to quantum datasets may now be developed, thanks to this method that tackles PCA diagonalization and enables deployments on datasets like MNIST and molecular ground states [10]. An enhanced version of the approach that utilized a resonant QPCA methodology with minimal additional qubits was later developed. The resource-efficient DR for ML problems was demonstrated by this invention, which achieved 86% efficiency and 90% fidelity [11].

Another study highlights two areas where quantum computing might be advantageous for ML: generative models and unsupervised learning. The problems, like noise and restricted qubit connection, are brought to light, and in order to address them, hybrid solutions like the Quantum-Assisted Helmholtz Machine (QAHM) are suggested [12]. The last couple of years watershed moment for QML, evidenced by a massive benchmarking study that evaluated 12 quantum models on 160 datasets. It is crucial to conduct a comprehensive experimental design and evaluation in QML research since, surprisingly, classical models are typically superior to quantum classifiers [13]. In healthcare, QML models like Quantum Support Vector Machines (QSVM) and QNN showed transformative potential. Studies demonstrated improvements of 20%-30% in disease segmentation, medical imaging, and bio-signal analysis accuracy, underlining QML's applicability in genomic sequencing and diagnostics [14, 15]. In financial fraud detection, QSVM achieved superior F1 scores of 0.98 for fraud and non-fraud classes, showcasing QML's ability to handle complex classification tasks in high-stakes industries [16].

Moreover, QML's integration with engineering applications, such as wind turbine pitch fault detection, demonstrated superior performance. Quantum models achieved a mean accuracy of 92.5%, outperforming traditional ML models like random forests and k-nearest neighbors [17].The paper introduces the Quantum Variational Classifier and Quantum Kernel Estimator, leveraging quantum Hilbert space to enhance supervised learning, achieving notable accuracy improvements and demonstrating quantum advantage in ML [18]. Another study introduced self-adaptive quantum kernel (SAQK) PCA as an advanced approach for enhancing information retention. The findings illustrate that SAQK PCA surpasses classical PCA in a number of back-end ML tasks, particularly in low-dimensional circumstances with constrained access to quantum bits [19]. Beyond specific applications, encoding schemes and hybrid architectures emerged as vital research areas. One study showcased quantum classifiers that achieved competitive performance in the Fashion-MNIST classification with as few as 11 qubits, demonstrating reduced qubit requirements and enhanced scalability for quantum models [20].

Despite these advancements, challenges persist. Critical evaluations revealed that the exponential speedups claimed by QPCA heavily depend on state preparation assumptions, emphasizing the need for practical encoding methods and efficient state preparation protocols [21]. Additionally, QML applications in data mining and cloud environments showed improvements in scalability, memory utilization, and robustness, driven by QPCA and feature reduction techniques [22]. In wireless communications, QML algorithms optimized performance using quantum-enhanced search and reinforcement learning methods [23]. Biomedical research further explored QML's potential, with algorithms like QSVM and QNN achieving significant accuracy improvements in genomic sequencing, bioinformatics, and medical imaging [24, 25].

In [26], "Classical-to-Quantum Knowledge Distillation," the authors sought to improve QNNs by using pre-trained classical CNNs. To train 4-qubit and 8-qubit PQCs on typical datasets like MNIST, FashionMNIST, and CIFAR10, they specifically used conventional CNN models like AlexNet, LeNet, ResNet, DenseNet, and EfficientNet. Accuracy boosts of about 7.49% on MNIST, 3.25% on FashionMNIST, and 3.69% on CIFAR10 were achieved using knowledge distillation, according to their data. Out of all the methods they examined, amplitude-encoding approaches produced the best results for data encoding and completely linked layers for DR.

A hybrid quantum-classical method for efficiently solving eigenvalue problems using quantum hardware, the Variational Quantum Eigensolver (VQE) was thoroughly studied theoretically by [27]. They made algorithmic advancements that improved accuracy and resource efficiency, like the variational adiabatic ansatz and the unitary coupled-cluster (UCC) approaches. For the purpose of reducing inherent errors in quantum devices in the near future, they also suggested quantum variational error suppression. Their methodological advancements led to substantial decreases in computational cost, such as derivative-free optimisation and Hamiltonian averaging.

These advancements highlight QML's transformative potential in addressing computationally complex problems across industries. In spite of persistent restrictions imposed by encoding protocols and technology, the quantum algorithm revolution promises major progress, propelling innovation in data-heavy industries like medical care, financial services, and engineering.

3. Methodology

3.1. Dataset Description

This study worked with the **Wisconsin Breast Cancer Dataset** [28], **Banknote Authentication Dataset** [29] and the **DARWIN Dataset** [30] to evaluate the efficacy of the suggested technique. The diverse designs and properties of these datasets allowed for a comprehensive evaluation of QML algorithms and algorithms influenced by quantum mechanics.

Wisconsin Breast Cancer Dataset

Digital pictures of breast tumor fine-needle aspirates were utilized to produce 30 numerical parameters for the 569 patients included in the Wisconsin Breast Cancer Dataset. These characteristics represent several characteristics of cell nuclei, including their radius, texture, smoothness, and concavity. Labels in this dataset indicate if the tumor is benign (label: 0) or malignant (label: 1), providing a binary classification. Due to its extensive feature set and balanced distribution, it is commonly used in biomedical ML tasks [28].

Banknote Authentication Dataset

One thousand three hundred seventy-two examples of real and fake banknotes, along with four numerical characteristics, make up the Banknote Authentication Dataset. Features like entropy, skewness, and variance are statistical assessments of wavelet-transformed pictures. The labels in the dataset indicate if a banknote is authentic (label: 1) or forged (label: 0). The dataset is binary. It is used as a standard for financial data analytics categorization tasks [29].

DARWIN Dataset

The DARWIN dataset captures handwriting characteristics used to differentiate between healthy individuals and patients with Alzheimer's disease. It includes various numerical features that describe pen dynamics such as pressure, speed, and stroke patterns. The dataset provides binary classification labels indicating either a healthy state or cognitive impairment. Owing to its detailed representation of motor function, it is commonly applied in biomedical ML studies for early diagnosis of neurodegenerative disorders [30].

Table 1: Summary of Dataset Characteristics

Dataset	Instances	Features	Feature Type	Labels
Wisconsin Breast Cancer	569	30	Numerical	Benign (0), Malignant (1)
Banknote Authentication	1,372	4	Numerical	Authentic (1), Forged (0)
DARWIN	174	451	Numerical	Patient (1), Healthy (0)

To guarantee data consistency and relevance for classification tasks, the datasets were subjected to many preprocessing stages, including normalization, label encoding, managing missing values, and feature selection. A chi-square test was used to assess the statistical dependency between each characteristic and the target class label, in order to determine which features were most useful for classification. This technique measures the dissimilarity between observed and predicted distributions under the independence assumption. Features are thought to be more useful for predicting the target variable if their chi-square scores are greater. After determining the relationship between the target variable Y and a specific attribute X, the chi-square statistic is computed using Eq. (1).

$$\chi^2 = \sum_{i=1}^{n} \sum_{j=1}^{m} \frac{\left(O_{ij} - E_{ij}\right)^2}{E_{ij}}, \tag{1}$$

Where O_{ij} is the observed frequency for feature i and class j, E_{ij} is the expected frequency, which is calculated followed by Eq. (2).

$$E_{ij} = \frac{\text{Row Total}_i \cdot \text{Column Total}_j}{\text{Grand Total}}. \tag{2}$$

The Chi-Square test evaluates the null hypothesis H_0 that the feature X is independent of the target Y. A higher χ^2 value indicates a stronger association between the feature and the target [31]. The feature selection process is described as follows:

I. **Input:** Preprocessed datasets with k features.

II. **Chi-Square Test:** For each feature X_i, compute the Chi-Square statistic with respect to the target variable Y.

III. **Rank Features:** Rank all features based on their χ^2 scores in descending order.

IV. **Select Prominent Features:** Retain the top 4 features with the highest χ^2 scores for both datasets:

- **Wisconsin Breast Cancer Dataset:** Features selected include `radius_worst, concave points_worst, radius_mean` and `perimeter_mean`.
- **Banknote Authentication Dataset:** All 4 features (`variance, skewness, kurtosis` and `entropy`) were retained since the dataset inherently has 4 features.
- **DARWIN Dataset:** Features selected include `num_of_pendown23`, `num_of_pendown19`, `num_of_pendown18`, and `num_of_pendown4`.

This process reduces dimensionality while ensuring the retained features have strong predictive power, facilitating efficient learning and improved model performance. To check if this choice is needed and how it affects results, we conduct tests comparing performance using χ^2 filtering, both classical PCA and KPCA, quantum PCA, and QVAE. Due to limited computing resources and the complicated nature of quantum state tomography, this process only allows up to four input variables and demonstrates that reducing features before QPCA maintains acceptable performance while respecting computational constraints.

3.2. Classical and Quantum Data

Classical data, characterized by its deterministic representation as binary bits, text, numerical values, or images, serves as the foundation for traditional ML algorithms. Such data is processed using classical computational methods that rely on well-defined states and deterministic operations [32]. In contrast, quantum data is generated from quantum mechanical systems and is encoded in qubits, leveraging fundamental quantum properties such as entanglement and superposition. This allows quantum information to exist in probabilistic and highly correlated forms [33].

A high-dimensional Hilbert space, where quantum states are formally represented as vectors, is where quantum data resides because of its uniquely quantum nature. The mathematical form provides a clear and expressive way to deal with high-dimensional data, making it easier to encode complex correlations and linkages [34]. Within the Hilbert space framework, quantum algorithms use linear transformations, such as unitary operations, to perform computations. These algorithms are capable of achieving exponential scalability and computational speedups for certain tasks like pattern recognition, optimization, and sampling [1].

Table 2: Assessment of the Features of Classical and Quantum Data

Aspect	Classical Data	Quantum Data
Basic Unit	**Bit:** The binary value of a bit is either 0 or 1.	**Qubit:** A qubit can contain the values 0 and 1, or even a superposition of both, all at once.
State Representation	Only a single state at a time, either 0 or 1.	The possibility of existing in a superposition of states is represented as a vector in two dimensions.
Initialization	Initialized as 0 or 1.	Typically initialized as 0.
Dimensionality	A single binary digit.	A pair of floating-point numbers.
Encoding	Data is encoded in binary form, utilizing values such as voltage levels and magnetic polarization.	Data is encoded in quantum states through the characteristics of particles, such as spin, polarization, or energy levels.
Computation Models	Simple circuits that use classical logic gates such as AND, OR, and NOT.	Quantum circuits with gates like Pauli-X, Y, Z, Hadamard, CNOT, and phase shift.
Physical Hardware	Constructed with transistors, semiconductors, and traditional electronic components.	Constructed using superconducting circuits, trapped ions, photons, or other quantum systems.
Read Operation	Deterministic: Always 0 or 1.	Probabilistic: Collapses to 0 or 1 upon measurement.

The introduction of stochasticity into quantum measurements, owing to their probabilistic character, can open up new avenues for data generation and pattern recognition that traditional computing approaches simply cannot match [35]. At present, there are significant challenges with quantum data encoding, manipulation, and measurement, particularly with quantum environments that are loud and prone to errors, which hinders their scalability [36]. It is necessary to enhance hardware stability, noise reduction, and error correction in order to properly address the difficulties.

New studies have shown that quantum data might be useful for ML. To illustrate the point, studies on quantum embeddings have demonstrated how transforming classical data into quantum states may enhance feature extraction and data separability, leading to more accurate ML models [37]. Studying quantum encoding of classical data in comparison has shown how important it is to correctly prepare quantum states to enable quantum-based learning techniques [38]. Novel computational methodologies for a broad array of scientific and technological applications are opened up by the groundbreaking role of merging ML with quantum data and the tight mathematical structure of Hilbert space.

As a combined field, the two disciplines are fundamental to QML. One may combine ML with QC in four different ways, which is demonstrated in Figure 1:

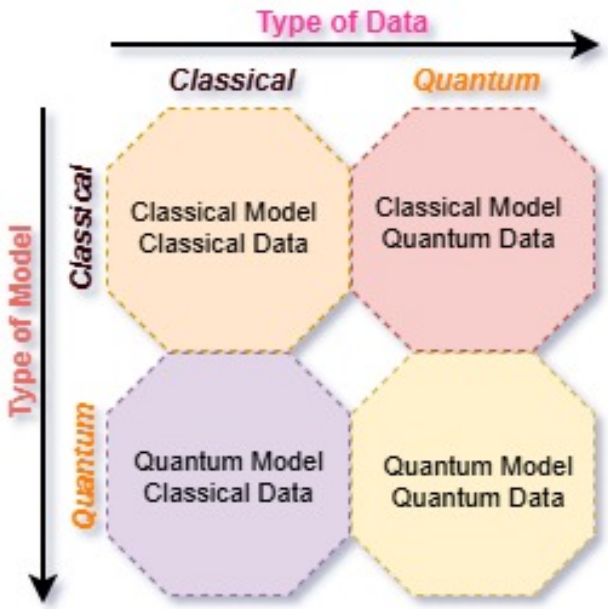

Figure 1: Classification of Models Based on Data and Computational Frameworks.

- **Classical-Classical approach (CC):** This method uses traditional approaches rooted in quantum computing, quantum physics, and quantum information theory. These algorithms, which are said to be "inspired by quantum mechanics," are implemented using conventional methods and data on physical computers.
- **Classical-Quantum approach (CQ):** The goal of this approach is to do effective ML with classical data by applying quantum ML algorithms. In this context, the usual intention is to find quantum algorithms that can perform ML tasks more effectively than classical algorithms or to find quantum versions of popular conventional algorithms.
- **Quantum-Classical approach (QC):** Here, quantum computers are able to learn and gain crucial insights from quantum data by applying traditional ML methods and algorithms to it.
- **Quantum-Quantum approach (QQ):** Quantum algorithms and data are at the heart of this method. To rephrase, QML algorithms access the data by manipulating quantum states to learn about the patterns at work.

3.3. Basic Quantum Gates

The computer industry heavily relies on the circuit framework of a computer for designing and building actual computing hardware, as it provides the most usable abstraction of the computing process. In the quantum circuit

model of computing, the quantum gate is the basic quantum circuit that works with qubits. Like the classical logic gate, qubits are the core elements of quantum circuits that is mention in Table 3. Each and every one of the quantum gates can be turned back on and off, unlike classical logic gates. Hence, unitary matrices [39], stand in for quantum gates. This ensures that the circuits' quantum gates never change their input and output counts. To change one quantum state into another, operators known as quantum gates use unitary matrices to operate on the original quantum state.

Table 3: Comparison of Quantum Gates and Their Classical Analogues

Quantum Gate	Input	Classical Gate	Matrix	Short Description
Pauli-X gate	1 qubit	Not gate	$X = \begin{bmatrix} 0 & 1 \\ 1 & 0 \end{bmatrix}$	Rotates the qubit state about the x-axis.
Pauli-Y gate	1 qubit	None	$Y = \begin{bmatrix} 0 & -i \\ i & 0 \end{bmatrix}$	Rotates the qubit state about the y-axis.
Pauli-Z gate	1 qubit	None	$Z = \begin{bmatrix} 1 & 0 \\ 0 & -1 \end{bmatrix}$	Rotates the qubit state about the z-axis, which is a subtype of the phase shift gate.
Hadamard gate	1 qubit	None	$H = \frac{1}{\sqrt{2}} \begin{bmatrix} 1 & 1 \\ 1 & -1 \end{bmatrix}$	Establish a superposition.
Phase shift	1 qubit	None	$S = \begin{bmatrix} 1 & 0 \\ 0 & e^{i\phi} \end{bmatrix}$	It does not change the basis state $\|0\rangle$ and maps $\|1\rangle$ to $e^{i\phi}\|1\rangle$.
Controlled Not gate	2 or more qubits	Not gate	$CNOT = \begin{bmatrix} 1 & 0 & 0 & 0 \\ 0 & 1 & 0 & 0 \\ 0 & 0 & 0 & 1 \\ 0 & 0 & 1 & 0 \end{bmatrix}$	It uses 2 qubits, and when the control qubit is set, only then does it execute the NOT operation on the target qubit.
SWAP	2 qubits	None	$SWAP = \begin{bmatrix} 1 & 0 & 0 & 0 \\ 0 & 0 & 1 & 0 \\ 0 & 1 & 0 & 0 \\ 0 & 0 & 0 & 1 \end{bmatrix}$	It has an effect on 2 qubits by switching their states.

3.4. Principal Component Analysis and Kernel Principal Component Analysis

PCA is a classical linear DR technique that projects data onto a lower-dimensional subspace by maximizing variance retention [40]. For a centered dataset $\mathbf{X} \in \mathbb{R}^{n \times d}$ with n samples and d features, the covariance matrix is computed as Eq. (3)

$$\mathbf{C} = \frac{1}{n-1}\mathbf{X}^\top \mathbf{X} \tag{3}$$

The principal components correspond to the top-k eigenvectors $\mathbf{W} \in \mathbb{R}^{d \times k}$ associated with the largest eigenvalues of $\mathbf{C}$. The reduced data representation is obtained by projection:

$$\mathbf{Z} = \mathbf{X}\mathbf{W} \tag{4}$$

PCA is computationally efficient but assumes linear relationships within the data. On the other hand, KPCA extends PCA to nonlinear data by implicitly mapping inputs into a high-dimensional feature space $\mathcal{F}$ via a nonlinear mapping

$\phi : \mathbb{R}^d \to \mathcal{F}$ [41]. The kernel trick avoids explicit computation of ϕ by using a kernel function that is mention in Eq. (5)

$$k(\mathbf{x}_i, \mathbf{x}_j) = \langle \phi(\mathbf{x}_i), \phi(\mathbf{x}_j) \rangle, \tag{5}$$

forming the kernel matrix $\mathbf{K} \in \mathbb{R}^{n \times n}$ with entries $\mathbf{K}_{ij} = k(\mathbf{x}_i, \mathbf{x}_j)$. Eigendecomposition of the centered kernel matrix yields principal components in $\mathcal{F}$, enabling nonlinear DR at increased computational cost.

PCA is suitable for linear data with lower computational demand, whereas KPCA captures complex nonlinear structures but requires higher computational resources. The choice depends on data characteristics and computational considerations.

3.5. Quantum Principal Component Analysis(QPCA)

PCA is a well-established strategy for classical data analysis, widely employed in tasks like DR, feature extraction, data visualization, and data compression [40]. However, as the volume and dimensionality of data continue to grow exponentially, classical PCA faces scalability challenges due to the computational cost of eigenvalue decomposition on large covariance matrices [42].

Recent breakthroughs in quantum computing have paved the way for exciting new possibilities in data analysis and DR techniques [43, 44]. QPCA is a quantum algorithm that, for specific problem instances with efficient state preparation, offers the potential for exponential speed-up over its classical counterpart by efficiently estimating the principal components of high-dimensional datasets. [45].

QPCA emerges as a quantum counterpart to PCA, leveraging the inherent parallelism and computational advantages of quantum mechanics to address classical limitations of PCA [46]. An essential concept underlying QPCA is represented in Figure 2, which has the data matrix as a quantum state and then use quantum algorithms such as quantum phase estimation to directly obtain the principal components, without the need for eigenvalue decomposition [47].

In this work, we investigate the QPCA algorithm proposed in the literature [48, 49].

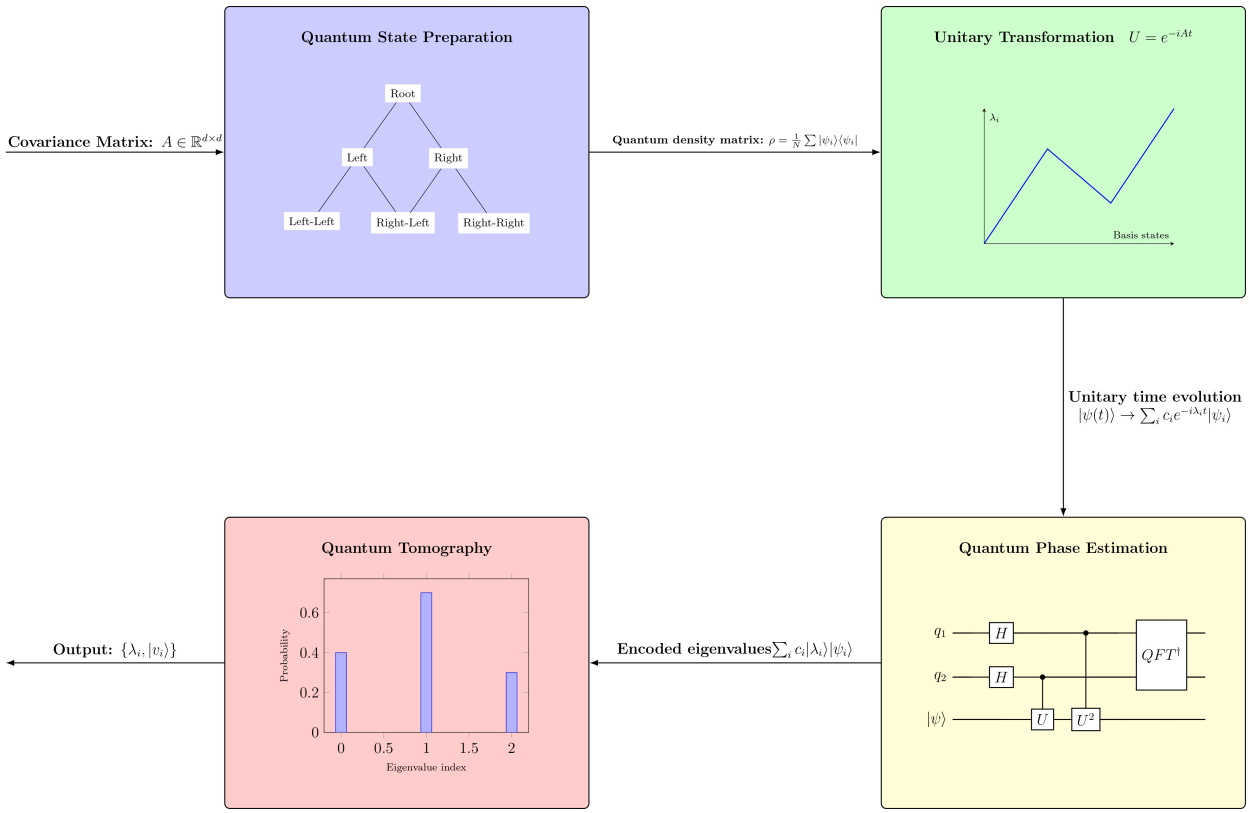

Figure 2: Methodology of Quantum Principal Component Analysis.

Quantum State Preparation via Hierarchical Amplitude

In this step, we encode classical data to quantum states, which involves translating a matrix into a normalized quantum representation using a hierarchical binary tree. The matrix elements are squared and normalized to form probabilities, ensuring $\sum_{i,j} |\psi_{ij}|^2 = 1$. Each tree node represents the square root of its children's summed probabilities, and angles (θ) for quantum circuit parameterization are computed by Eq. (6).

$$\theta_{\text{right}} = 2 \arccos\left(\frac{\text{Right Child}}{\text{Parent}}\right), \quad \theta_{\text{left}} = 2 \arcsin\left(\frac{\text{Left Child}}{\text{Parent}}\right) \tag{6}$$

The computed thetas provide the necessary rotation angles to encode the original matrix into the quantum state.

Unitary Transformation for Quantum Phase Estimation

Here, we construct the unitary operator e^{-iAt} that is used to extract eigenvalues through quantum phase estimation (QPE) and the practical speed-up depends on the sparsity of A. Here, A is the covariance matrix acts as the Hamiltonian and e^{-iAt} evolves the quantum state, encoding eigenvalues as phases represented by Eq. (7).

$$e^{-iAt}|\psi\rangle \rightarrow e^{-i\lambda t}|\psi\rangle \tag{7}$$

where λ is an eigenvalue. By assuming multiple copies of A and using its low rank structure, e^{-iAt} is approximated with precision ϵ in $O(\text{polylog}(1/\epsilon))$. This allows efficient decomposition into quantum gates, enabling scalable eigenvalue extraction. Thus, after the unitary operation, the quantum states are represented in Eq. (8).

$$|\psi(t)\rangle \rightarrow \sum_i c_i e^{-i\lambda_i t}|\psi_i\rangle \tag{8}$$

Quantum Phase Estimation for Eigenvalue Extraction

Quantum phase estimation (QPE) is an essential component of QPCA to extract the eigenvalues of a matrix. Using n-qubits (resolution), QPE approximates eigenvalues λ_i with precision 2^{-n}. Given an initial state $|\psi(t)\rangle = \sum_i c_i e^{-i\lambda_i t}|\psi_i\rangle$, the circuit transforms it to:

$$|\psi(t)\rangle \rightarrow \sum_i c_i|\lambda_i\rangle|\psi_i\rangle \tag{9}$$

where $|\lambda_i\rangle$ encodes the eigenvalues in Eq. (9). Measurement of the circuit state vector produces eigenvalues through bitstring analysis, allowing efficient extraction of principal components in QPCA.

Eigenvalue and Eigenvector Extraction via Quantum Tomography

Eigenvalue and eigenvector extraction utilizes a quantum tomography-based approach. After Quantum Phase Estimation (QPE), the eigenvalues λ_i are encoded in the least significant qubits, with the probability of each state $|\lambda_i\rangle$ corresponding to the magnitude squared of the amplitude. From Eq. (10), these eigenvalues are derived.

$$\lambda_i = \frac{\text{int}(\text{binary state}, 2)}{2^{\text{resolution}}} \tag{10}$$

The probabilities associated with each state are aggregated for degenerate eigenvalues, and the corresponding eigenvector components are extracted from the amplitudes of the quantum states. The normalization of each eigenvector $\mathbf{v}$ is achieved by scaling the amplitudes using Eq. (11).

$$\|\mathbf{v}\|^2 = \sum_i |a_i|^2 = 1 \tag{11}$$

Sign estimation, similar to quantum tomography, resolves the relative signs of eigenvector components by utilizing quantum interference. A controlled operation applied to the quantum states allows the extraction of signs, and the reconstructed eigenvector $\mathbf{v}$ is shown in Eq. (12).

$$\mathbf{v} = \sum_i a_i|\psi_i\rangle \cdot \text{sign}(a_i) \tag{12}$$

where a_i are the amplitudes of the components of the eigenstate. This procedure, rooted in quantum tomography, extracts both the eigenvalues and the eigenvectors with high precision and minimal resource overhead, enabling scalable and accurate PCA in QPCA.

3.6. *Quantum Variational Autoencoder (QVAE)*

Quantum Variational Autoencoders (QVAEs) are an advanced extension of the classical Variational Autoencoder (VAE) framework, designed to grasp the unique computational advantages of quantum systems for encoding and decoding data. By integrating quantum circuits into the architecture, QVAEs address challenges faced by classical VAEs, such as scalability in high-dimensional tasks, by utilizing the exponentially large Hilbert space of quantum systems. At their core, QVAEs combine the probabilistic generative capabilities of VAEs with quantum mechanics to efficiently model and process vast and complex data distributions [50, 48].

In classical VAEs, the encoding process maps input data x to a probabilistic latent representation z, approximating the posterior distribution $Q(z|x)$. The loss function for VAEs, known as the Evidence Lower Bound (ELBO), is mentioned in Eq. (13).

$$L_{\text{VAE}} = \mathbb{E}_{Q(z|x)}\left[\log P(x|z)\right] - D_{\text{KL}}(Q(z|x)\|P(z)) \tag{13}$$

where $P(x|z)$ is the likelihood of reconstructing x from z, and D_{KL} represents the Kullback-Leibler divergence that aligns $Q(z|x)$ with the prior distribution $P(z)$ [50].

In QVAEs, the latent representation z is replaced by a quantum state $|z\rangle$, enabling efficient representation of high-dimensional data using quantum amplitudes. The encoder maps input data x into this quantum latent state:

$$|z\rangle = U_{\text{encoder}}(x)|0\rangle \tag{14}$$

where $U_{\text{encoder}}(x)$ is a parameterized quantum circuit acting on the initial state $|0\rangle$ [51]. The decoder reconstructs the input data by applying another parameterized quantum circuit to $|z\rangle$:

$$\tilde{x} = U_{\text{decoder}}(|z\rangle) \tag{15}$$

where $\tilde{x}$ represents the reconstructed data.

The quantum ELBO extends the classical formulation to include quantum probabilities:

$$L_{\text{QVAE}} = \mathbb{E}_{Q_\theta(|z\rangle|x)}\left[\log P_\phi(x||z\rangle)\right] - D_{\text{KL}}(Q_\theta(|z\rangle|x)\|P(|z\rangle)) \tag{16}$$

where $Q_\theta(|z\rangle|x)$ is the distribution of the quantum encoder in the quantum latent states, $P_\phi(x||z\rangle)$ is the likelihood of reconstructing x given the quantum latent state, $P(|z\rangle)$ is the prior distribution, often chosen as a uniform or Gaussian quantum state [52].

This study uses the QVAE technique to represent a novel approach to DR using quantum circuits to extract lower-dimensional representations of high-dimensional data. The process begins by encoding input data $X = [x_1, x_2, \ldots, x_n]$, where each feature x_i is transformed into a quantum state. This is achieved through the application of $R_y(x_i)$ rotations, which map each feature onto a corresponding qubit. This encoding is mathematically expressed in Eq. (17).

$$|\psi_i\rangle = R_y(x_i)|0\rangle = \cos\left(\frac{x_i}{2}\right)|0\rangle + \sin\left(\frac{x_i}{2}\right)|1\rangle \tag{17}$$

thereby ensuring the quantum representation of the input dataset.

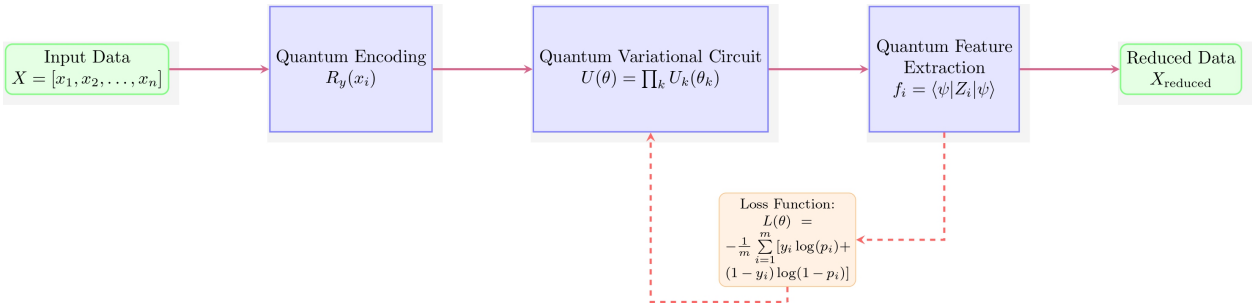

Figure 3: Methodology of Quantum Variational Autoencoder.

Applying a variational quantum circuit to the quantum state follows the encoding step. For this circuit, the set of parameters optimized during training is denoted by θ, and the unitary training operations are denoted by $U(\theta)$. Because of the entanglement and nonlinearity introduced by these actions, the quantum state undergoes a transformation:

$$|\psi_{\text{encoded}}\rangle = U(\theta)|\psi\rangle \tag{18}$$

In order to increase the variational circuit's representational capacity, structured layers like StronglyEntanglingLayers are usually used for implementation. These layers contain parameterized gates and entanglement operations.

Through the measurement of Pauli-Z operators on individual qubits, pertinent aspects of the quantum state may be extracted, leading to DR. It is technically possible to describe the reduced features mathematically as:

$$f_i = \langle\psi_{\text{encoded}}|Z_i|\psi_{\text{encoded}}\rangle \tag{19}$$

where i represents the qubits that were measured. The two-dimensional feature vector that results from using two qubits for measurement preserves crucial details from the initial high-dimensional dataset.

In order to optimize the encoder, a binary cross-entropy loss function is employed. A linear combination of the retrieved characteristics is used to forecast the output labels, with the prediction for each sample provided by Eq. 20.

$$p_i = \sigma(f_1 + f_2) \tag{20}$$

where the sigmoid function is represented by σ and the features f1 and f2 are the average values of the Pauli-Z operator as measured on the first and second qubits of the encoded quantum state, respectively. Also, the loss function is expressed as:

$$L(\theta) = -\frac{1}{m}\sum_{i=1}^{m}\left[y_i \log(p_i) + (1 - y_i)\log(1 - p_i)\right] \tag{21}$$

Where y_i is the actual label, and p_i is the expected likelihood. To optimize θ, one iteratively minimizes the loss function by descending the gradient or using other optimization techniques.

The feature sets of the test and training datasets are trimmed by the quantum encoder immediately following the training. The structure and important aspects of the original data are successfully conserved in the reduced dataset X_{reduced}, even though its dimensionality is lowered. By providing a robust and effective approach to DR and feature extraction, this method showcases the potential of QC to address challenges in high-dimensional analysis of data.

*3.7. **Support Vector Machines (SVM)***

An SVM is a supervised ML algorithm used to find the optimal hyperplane to partition data points into discrete classes in a high-dimensional space. In the case of data that can be easily separated into classes, SVM finds the hyperplane that maximizes the margin. This margin is the distance between the hyperplane and the data points that are closest to each class, specifically the support vectors. This optimization problem can be represented mathematically in Eq. (22).

$$\min_{w,b} \frac{1}{2}\|w\|^2 \tag{22}$$

subject to:

$$y_i(w \cdot x_i + b) \geq 1, \quad \forall i, \tag{23}$$

Where w is the weight vector defining the hyperplane, b is the bias term, x_i represents the feature vectors, $y_i \in \{-1, 1\}$ are the class labels which is represented in Eq. (23). The solution to this problem provides the hyperplane with maximum margin [53].

Soft Margin SVM

To tackle noisy or overlapping data, SVM reveals slack variables (ξ_i) and a regularization parameter (C) to balance margin maximization with classification errors. This leads to the soft margin SVM, represented by Eq. (24).

$$\min_{w,b,\xi} \frac{1}{2}\|w\|^2 + C\sum_{i=1}^{N}\xi_i \tag{24}$$

subject to:

$$y_i(w \cdot x_i + b) \geq 1 - \xi_i, \quad \xi_i \geq 0, \quad \forall i, \tag{25}$$

where ξ_i measures the degree of misclassification for the i-th data point [54, 42].

Decision Function

Eq. (26) follows the final decision function for the classification of new data points.

$$f(x) = \text{sign}\left(\sum_{i=1}^{N}\alpha_i y_i(x_i \cdot x) + b\right), \tag{26}$$

where α_i are the Lagrange multipliers, x_i are the support vectors.This equation determines whether a new data point belongs to a specific class based on the support vectors and the learned hyperplane [42].

SVM has widespread applications in classification tasks such as text categorization, image recognition, and bioinformatics, where its capability to deal with high-dimensional data effectively makes it a popular choice [54].

3.8. ***Quantum Neural Network(QNN)***

QNNs combine the foundational principles of traditional artificial neural networks (ANNs) with quantum computational models, which offer potential advantages over classical ANNs. The perceptron represents the simplest ANN model, simulating synaptic connections in biological neurons by employing an input layer consisting of neurons $n_1, n_2, n_3, \ldots, n_m$ and a corresponding set of weights $w_1, w_2, w_3, \ldots, w_m$. The perceptron's output activates when the weighted sum of inputs surpasses a threshold θ, mathematically expressed as:

$$f(x) = \begin{cases} 0, & \text{if } \sum_{i=1}^{m} n_i w_i \leq \theta, \\ 1, & \text{otherwise.} \end{cases} \tag{27}$$

Here, $f(x)$ denotes the activation function. In ML, multilayer ANNs incorporating hidden layers introduce nonlinearity, allowing for more complex decision boundaries. During supervised learning, the network weights are iteratively updated based on the error between predicted and target outputs until convergence.

Despite the increasing sophistication of classical architectures such as convolutional neural networks (CNNs), generative adversarial networks (GANs), and long short-term memory networks (LSTMs) [25] the complexity and computational cost escalate with the number of layers, connections, and neurons. Given the rapidly growing data volumes, a paradigm shift toward novel computing models is imperative. Quantum computing and QNNs present a promising alternative to address these challenges.

The quantum neuron, a quantum analogue of the classical neuron, constitutes the fundamental building block of QNNs. It receives an amplitude- and phase-modulated quantum state as input and outputs another quantum state, with weights encoded as complex amplitudes. This operation can be described as

$$y = U\left(\sum_i w_{i,y}|x_i\rangle\right), \tag{28}$$

where U is an arbitrary operator representing the activation function, and $w_{i,y}$ are the associated weights.

Learning in the quantum perceptron follows the update rule [55]:

$$w_{i,y}(t+1) = w_{i,y}(t) + \eta(|d\rangle - |y\rangle)\langle x_i|, \tag{29}$$

where $|d\rangle$ is the target state, $|y\rangle$ is the neuron's current state, and η is the learning rate.

In our proposed model, the output is obtained as the expectation value of the Pauli-Z operator on the first qubit and subsequently rescaled to the interval $[0, 1]$ for probabilistic interpretation. Training was performed using the Gradient Descent Optimizer with a fixed learning rate of 0.01 over 20 epochs. The binary cross-entropy loss function was employed to quantify prediction error. Model performance was evaluated on a separate test set by computing classification accuracy with a decision threshold of 0.5.

Several QNN architectures have been explored recently. For instance, Tacchino et al. [56] demonstrated the application of QNNs with multi-layer activation functions for pattern recognition in lie detection, achieving improved detection rates. Similarly, Niu et al. [57] proposed a quantum convolutional neural network (quantum-CNN) for decentralized voice processing, reporting consistent and competitive results relative to classical neural networks. Overall, QNNs exhibit substantial potential as enhancements over classical approaches. However, a fully developed QNN framework that conclusively delivers a quantum advantage remains an active area of research.

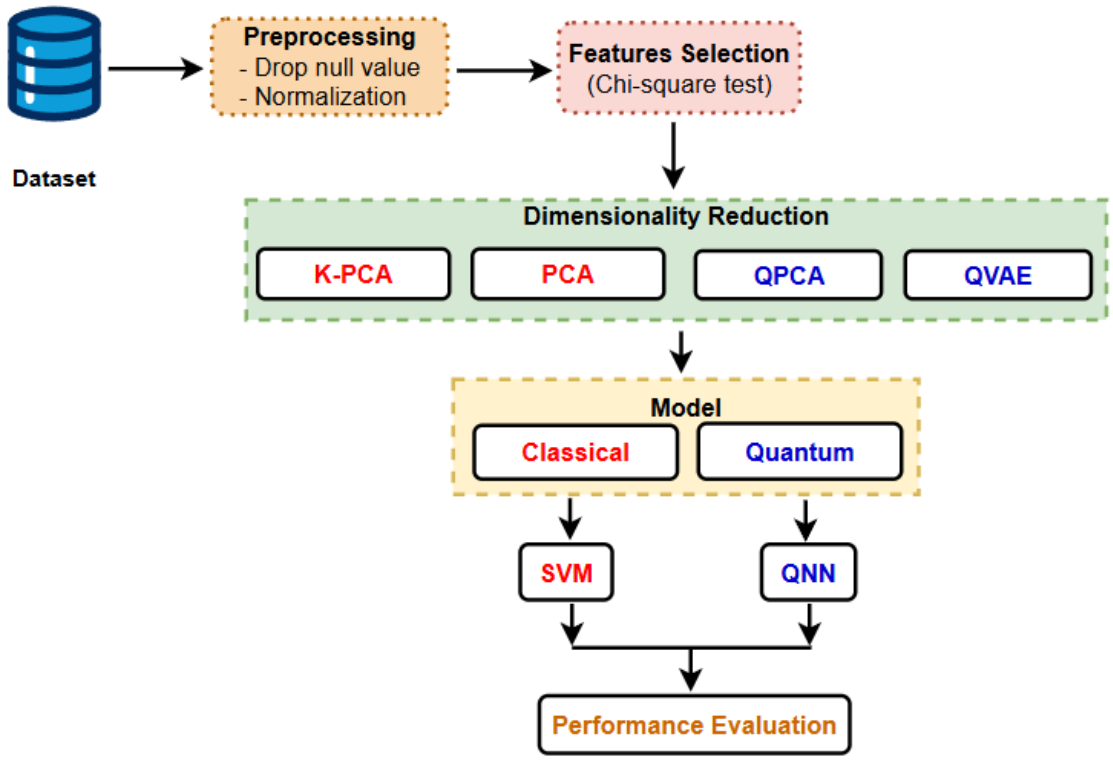

Figure 4: Workflow for Data Processing, Dimensionality Reduction, and Model Evaluation in Classical and Quantum Frameworks.

4. Results and Discussion

The outcomes of this study exhibit a comparison of classical and quantum approaches to DR and classification in different datasets. The impact of four distinct DR techniques on model performance was investigated: PCA,KPCA QPCA, and QVAE. We integrated these methods with SVM, QNN to demonstrate their efficacy on real-world classification tasks. The following discussion examines the results of several approaches, focusing on key performance metrics like precision, F1 score, recall, accuracy, and AUC.

4.1. Experimental Setups

The QPCA algorithm was implemented using the Qiskit framework (IBM Qiskit version 0.39.5). For the implementation of the QVAE and QNN, the PennyLane library (version 0.41.1) was utilized, leveraging its compatibility with multiple quantum simulators and hardware backends.

For the QPCA experiments, simulations were conducted on the Qiskit Aer QASM simulator backend with $80,000$ shots per circuit execution with resolution of 8. The high shot count and resolution ensure accurate estimation of quantum state tomography, which reconstructs the quantum state's density matrix from measurement outcomes. The quantum circuits for the QVAE and QNN were implemented using the PennyLane framework. The simulations utilized the *default.qubit* device, a state-vector simulator that provides a noise-free environment for developing and testing variational quantum circuits. Running the simulator was a computer system equipped with 8GB of RAM and an 8'th generation Core i5 processor.

4.2. Evaluation Metrics

The efficient functioning of the models was determined by applying the following parameters:

Accuracy: Accuracy is the proportion of events correctly classified in relation to the overall count of cases studied. It is demonstrated in Eq. (30).

$$\text{Accuracy} = \frac{\text{TP} + \text{TN}}{\text{TP} + \text{FP} + \text{TN} + \text{FN}} \tag{30}$$

In which the letters TP, TN, FP, and FN stand for True Positive, True Negative, False Positive, and False Negative, respectively.

Precision: Precision can be defined as the proportion of cases that have been accurately identified as positive in comparison to the total number of instances that have been anticipated to be positive. It indicates how certain we are that a predicted positive instance is actually positive:

$$\text{Precision} = \frac{\text{TP}}{\text{TP} + \text{FP}} \tag{31}$$

Recall: Recall is the proportion of true positive situations that are accurately recognized. It measures how accurately the model identifies all positive instances:

$$\text{Recall} = \frac{\text{TP}}{\text{TP} + \text{FN}} \tag{32}$$

F1-Measure: The F1-measure is considered to be the harmonic mean of the precision and recall measures, balancing their trade-off. Larger values indicate better model performance:

$$\text{F1-Measure} = 2 \cdot \frac{\text{Precision} \cdot \text{Recall}}{\text{Precision} + \text{Recall}} \tag{33}$$

Area Under the Curve (AUC): The AUC indicates how well the model can differentiate across categories. It stands for the region under the ROC curve, which stands for Receiver Operating Characteristic. Between 0.5 (complete discrimination) and 1.0 (random guessing), AUC values fall somewhere in the middle. Performance is improved with higher AUC values.

The results summarized in Tables 4 and 5 represent the comparative performance of classical and quantum methodologies for DR and classification across diverse datasets. The following discussion evaluates the efficacy of these approaches, emphasizing the DR techniques, model accuracy, and associated performance metrics.

Table 4: Comparison of Classical and Quantum Models for Different Dataset

Dataset Name	Feature Selection (Chi-Square test)	Dimensionality Reduction				Model Accuracy (%)	
		K-PCA	PCA	QPCA	QVAE	SVM	QNN
Breast Cancer	Yes	Yes	-	-	-	91%	93%
		-	Yes	-	-	94%	93%
		-	-	Yes	-	**95%**	91%
		-	-	-	Yes	94%	64%
BankNote	Yes	Yes	-	-	-	86%	85%
		-	Yes	-	-	82%	75%
		-	-	Yes	-	**98%**	91%
		-	-	-	Yes	86%	85%
DARWIN	Yes	Yes	-	-	-	63%	66%
		-	Yes	-	-	71%	69%
		-	-	Yes	-	**80%**	74%
		-	-	-	Yes	74%	70%

This study evaluated four DR techniques: PCA, KPCA, QPCA, and QVAE. Table 4 presents the comparative results of both classical SVM and QNN across multiple performance metrics. Notably, QPCA yielded the highest classification accuracy of 95% with a classical SVM on the Breast cancer dataset, whereas the QNN reached 91%. When employing PCA, the classical model attained 94% accuracy, marginally outperforming the QNN, which reached 93%. Conversely, KPCA facilitated superior performance for the QNN with 93% accuracy, exceeding the classical model's 91%. However, when QVAE was employed, the classical classifier maintained strong performance at 94%, while the QNN's accuracy decreased markedly to 64%.

In the Banknote dataset, the use of QPCA for DR yielded the highest accuracy of 98% for the classical model, whereas the QNN achieved 91%. When PCA was applied, the classical SVM attained 82% accuracy, outperforming the QNN, which achieved 75%. For both QVAE and KPCA DR methods, the classical SVM consistently achieved an accuracy of 86%, slightly exceeding the QNN's accuracy of 85%.

However, in the DARWIN dataset, using QPCA for DR, the classical model achieved the highest accuracy of 80%, compared to 74% for the QNN. With PCA, the classical SVM outperformed the QNN, achieving 71% accuracy versus 69%. When applying the QVAE, the classical SVM again slightly surpassed the QNN, reaching 74% accuracy compared to 70%. In contrast, KPCA enabled the QNN to outperform the classical SVM, with accuracies of 66% and 63%, respectively.

Table 5: Performance Metrics for Best Performing Model

Dataset	Precision	Recall	F1-Score	Accuracy	AUC
Breast Cancer	0.97	0.97	0.97	0.97	0.97
Bank Note	0.98	0.98	0.98	0.98	0.97
DARWIN	0.80	0.81	0.80	0.80	0.81

Table 5, summarizes the performance of the most effective models across all datasets, exhibiting superior predictive capabilities with consistently high accuracy, precision, recall, F1-score, and area under the curve (AUC) metrics. For the Breast cancer dataset, all evaluated metrics—precision, recall, F1-score, accuracy, and AUC—reached 0.97. Similarly, the Banknote dataset demonstrated metrics of 0.98 across precision, recall, F1-score, and accuracy, with a slightly lower AUC of 0.97. In the DARWIN dataset, precision, F1-score, and accuracy attained 0.80, while recall and AUC were marginally higher at 0.81. These results underscore the efficacy of classical models employing QPCA for DR. Additionally, the consistently high AUC values of 0.97 for the Breast cancer and banknote datasets affirm the

robust discriminative power of these models in classification tasks. The confusion matrix corresponding to different datasets is shown in Figure 5, and the accuracy graphs for our model appear in Figure 6, 7, and 8, respectively.

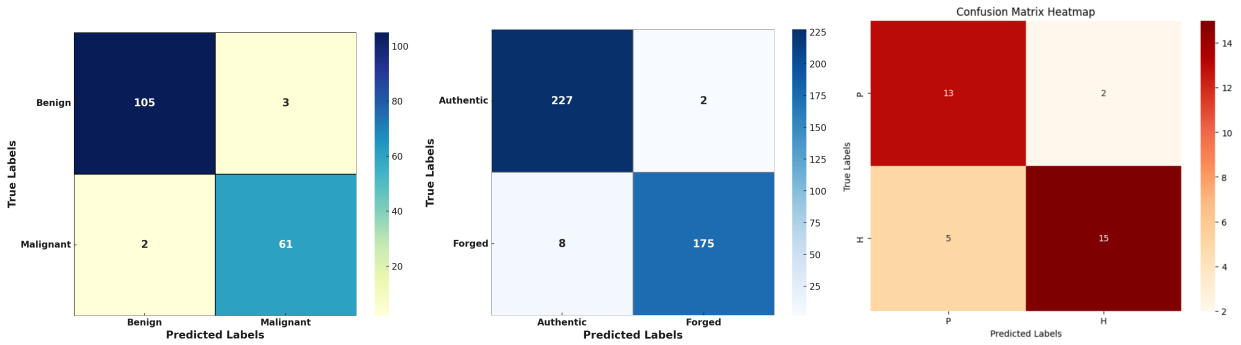

(a) Wisconsin Breast Cancer Dataset (b) Banknote Authentication Dataset (c) DARWIN Dataset

Figure 5: Confusion matrices for the best performing model on three datasets: (a) Wisconsin Breast Cancer, (b) Banknote Authentication, and (c) DARWIN.

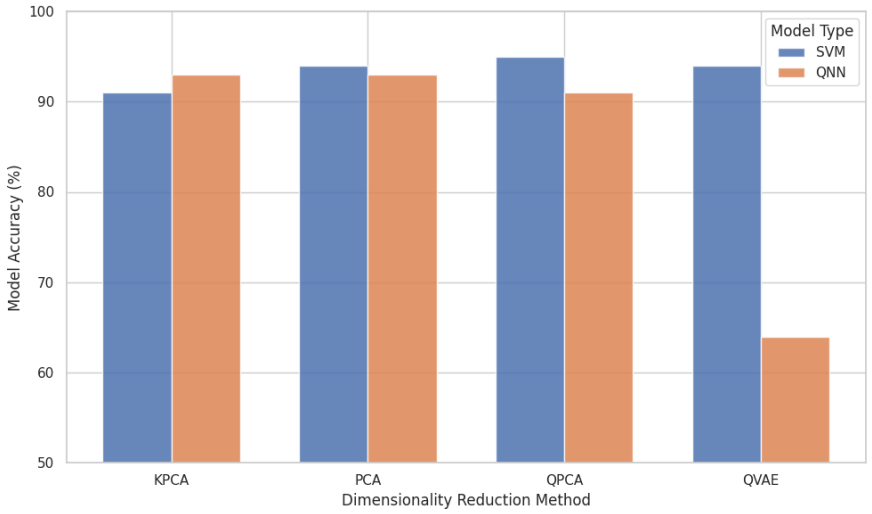

Figure 6: Model Accuracy for Wisconsin Breast Cancer Dataset.

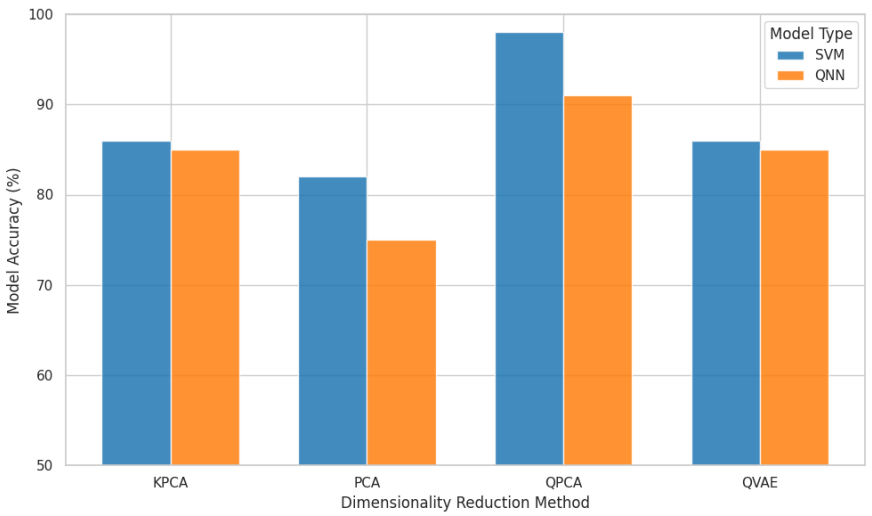

Figure 7: Model Accuracy for Banknote Authentication Dataset.

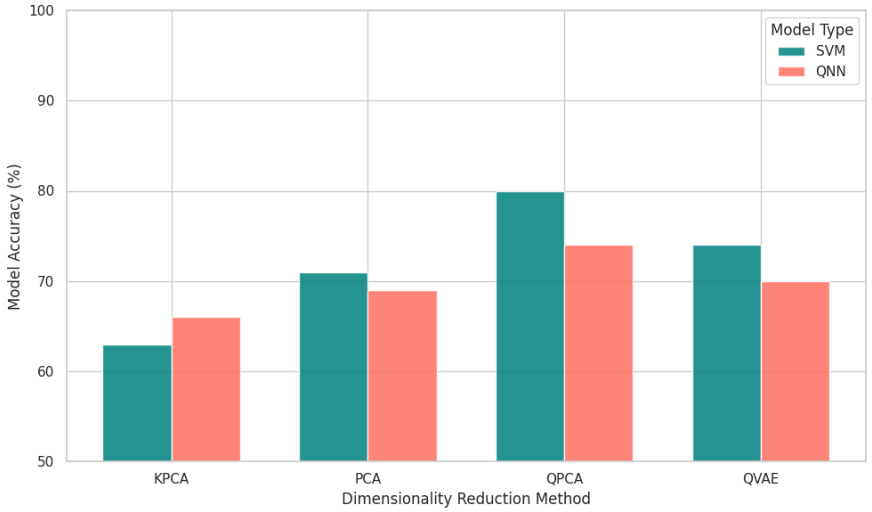

Figure 8: Model Accuracy for DARWIN Dataset.

5. Conclusion

This study highlights the profound potential of QC to revolutionize ML workflows by addressing the constraints of traditional approaches in the management of datasets of high dimensions. By integrating classical and quantum methodologies, considering PCA, KPCA, QPCA, and QVAE, the research demonstrates a classical framework capable of enhancing DR and improving computational efficiency. Comparative analysis across benchmark datasets reveals that while classical SVM models remain robust and dominant in terms of accuracy, quantum-enabled approaches such as QNNs showcase promising results. The classification accuracy for the suggested classical model was 95% in the Breast cancer dataset when QPCA was used, exceeding 91% for QNN. In contrast, in the Banknote and DARWIN datasets, the classical SVM approach produces an accuracy of 98% and 80%, while QNN produces 91% and 74%, respectively.The findings illustrate the viability of hybrid classical-quantum systems as a transformative paradigm in modern data science, capable of addressing computational bottlenecks inherent to large-scale datasets. Performance metrics and AUC values indicated that the classical SVM model outperformed other QML models. This study shows that quantum-enhanced DR effectively captures complex data features, outperforming classical methods at the preprocessing stage. However, when models are applied to the reduced data, classical ML algorithms achieve higher

accuracy, while quantum models deliver comparable results. These findings highlight the integrated powers of quantum and classical approaches in hybrid learning pipelines.This work not only establishes a foundational framework for integrating quantum computing into end-to-end ML pipelines but also emphasizes its potential to complement and extend the capabilities of traditional methods.

The quantum state tomography phase in QPCA is exponentially complex and computationally resource-constrained, hence our pipeline limits the input feature set to a maximum of four variables. So, we can't use more than four features (qubits) because it would need an excessive amount of measurements and computation time, which is beyond our CPU and runtime capabilities. In order to address these limitations and improve the overall performance of quantum models, researchers can look into using input features from more than four qubits in future studies.

Acknowledgement: We would like to acknowledge that there are no specific individuals or organizations to acknowledge for their contributions to this work.

Data Availability: The datasets used in this study are publicly available from the UCI ML Repository and can also be accessed through ML frameworks such as PyTorch or TensorFlow.

Funding Statement: There was no specific grant awarded for this study by public, private, or nonprofit funding organisations.

Conflicts of Interest: The authors declare that they have no conflicts of interest to report regarding the present study.

References

[1] J. Biamonte, P. Wittek, N. Pancotti, P. Rebentrost, N. Wiebe, S. Lloyd, Quantum machine learning, Nature 549 (7671) (2017) 195–202.

[2] G. T. Reddy, M. S. K. Reddy, K. Lakshmanna, R. Kaluri, D. Rajput, G. Srivastava, T. Baker, Analysis of dimensionality reduction techniques on big data, IEEE Access 8 (2020) 54776–54788. doi:10.1109/ACCESS.2020.2980942.

[3] Y. Li, R. gui Zhou, R. Xu, W. Hu, P. Fan, Quantum algorithm for the nonlinear dimensionality reduction with arbitrary kernel, Quantum Science Technology 6 (2020). doi:10.1088/2058-9565/abbe66.

[4] N. Gao, M. Wilson, T. Vandal, W. Vinci, R. Nemani, E. Rieffel, High-dimensional similarity search with quantum-assisted variational autoencoder, Proceedings of the 26th ACM SIGKDD International Conference on Knowledge Discovery Data Mining (2020). doi:10.1145/3394486.3403138.

[5] K. huan Yu, S. Lin, G. Guo, Quantum dimensionality reduction by linear discriminant analysis, Physica A: Statistical Mechanics and its Applications (2021). doi:10.1016/j.physa.2023.128554.

[6] A. Bellante, A. Luongo, S. Zanero, Quantum algorithms for svd-based data representation and analysis, Quantum Machine Intelligence 4 (2021).
URL https://api.semanticscholar.org/CorpusID:251263324

[7] C. He, J. Li, W. Liu, An exact quantum principal component analysis algorithm based on quantum singular value threshold, arXiv: Quantum Physics (2020).
URL https://api.semanticscholar.org/CorpusID:222124926

[8] C. He, J. Li, W. Liu, J. Peng, Z. J. Wang, A low-complexity quantum principal component analysis algorithm, IEEE Transactions on Quantum Engineering 3 (2022) 1–13.
URL https://api.semanticscholar.org/CorpusID:245729536

[9] T. Xin, L. Che, C. Xi, A. Singh, X. Nie, J. Li, Y. Dong, D. Lu, Experimental quantum principal component analysis via parametrized quantum circuits., Physical review letters 126 11 (2021) 110502.
URL https://api.semanticscholar.org/CorpusID:232775556

[10] M. H. Gordon, M. Cerezo, L. Cincio, P. J. Coles, Covariance matrix preparation for quantum principal component analysis, ArXiv abs/2204.03495 (2022).
URL https://api.semanticscholar.org/CorpusID:248006263

[11] Z. Li, Z. Chai, Y. Guo, W. Ji, M. Wang, F. Shi, Y. Wang, S. Lloyd, J. Du, Resonant quantum principal component analysis, Science Advances 7 (2021).
URL https://api.semanticscholar.org/CorpusID:233033364

[12] A. Perdomo-Ortiz, M. Benedetti, J. Realpe-Gómez, R. Biswas, Opportunities and challenges for quantum-assisted machine learning in near-term quantum computers, Quantum Science and Technology 3 (2017).
URL https://api.semanticscholar.org/CorpusID:3963470

[13] J. Bowles, S. Ahmed, M. Schuld, Better than classical? the subtle art of benchmarking quantum machine learning models, ArXiv abs/2403.07059 (2024).
URL https://api.semanticscholar.org/CorpusID:268364230

[14] D. Maheshwari, B. Garcia-Zapirain, D. Sierra-Sosa, Quantum machine learning applications in the biomedical domain: A systematic review, IEEE Access 10 (2022) 80463–80484.
URL https://api.semanticscholar.org/CorpusID:251189846

[15] U. Ullah, B. Garcia-Zapirain, Quantum machine learning revolution in healthcare: A systematic review of emerging perspectives and applications, IEEE Access 12 (2024) 11423–11450.
URL https://api.semanticscholar.org/CorpusID:267133956

[16] N. Innan, M. A.-Z. Khan, M. Bennai, Financial fraud detection: A comparative study of quantum machine learning models, ArXiv abs/2308.05237 (2023).
URL https://api.semanticscholar.org/CorpusID:260775542

[17] C. Correa-Jullian, S. Cofre-Martel, G. S. Martín, E. L. Droguett, G. de Novaes Pires Leite, A. B. R. Costa, Exploring quantum machine learning and feature reduction techniques for wind turbine pitch fault detection, Energies (2022).
URL https://api.semanticscholar.org/CorpusID:248144856

[18] V. Havlíček, A. D. Córcoles, K. Temme, A. W. Harrow, A. Kandala, J. M. Chow, J. M. Gambetta, Supervised learning with quantum-enhanced feature spaces, Nature 567 (7747) (2019) 209–212. doi:10.1038/s41586-019-0980-2.
URL http://dx.doi.org/10.1038/s41586-019-0980-2

[19] Z. Wang, T. van der Laan, M. Usman, Self-adaptive quantum kernel principal components analysis for compact readout of chemiresistive sensor arrays (2024). arXiv:2409.00115.
URL https://arxiv.org/abs/2409.00115

[20] R. Dilip, Y.-J. Liu, A. Smith, F. Pollmann, Data compression for quantum machine learning, Physical Review Research (2022).
URL https://api.semanticscholar.org/CorpusID:248377516

[21] E. Tang, Quantum principal component analysis only achieves an exponential speedup because of its state preparation assumptions., Physical review letters 127 6 (2018) 060503.
URL https://api.semanticscholar.org/CorpusID:236956378

[22] K. Sudharson, B. Alekhya, A comparative analysis of quantum-based approaches for scalable and efficient data mining in cloud environments, Quantum Inf. Comput. 23 (2023) 783–813.
URL https://api.semanticscholar.org/CorpusID:259950630

[23] B. Narottama, Z. Mohamed, S. Aïssa, Quantum machine learning for next-g wireless communications: Fundamentals and the path ahead, IEEE Open Journal of the Communications Society 4 (2023) 2204–2224.
URL https://api.semanticscholar.org/CorpusID:261319359

[24] G. Abdulsalam, S. Meshoul, H. Shaiba, Explainable heart disease prediction using ensemble-quantum machine learning approach, Intelligent Automation & Soft Computing (2023).
URL https://api.semanticscholar.org/CorpusID:252636995

[25] A. Jadhav, A. Rasool, M. Gyanchandani, Quantum machine learning: Scope for real-world problems, Procedia Computer Science 218 (2023) 2612–2625.

[26] M. J. Hasan, M. Mahdy, Bridging classical and quantum machine learning: Knowledge transfer from classical to quantum neural networks using knowledge distillation, arXiv preprint arXiv:2311.13810 (2023).

[27] J. R. McClean, J. Romero, R. Babbush, A. Aspuru-Guzik, The theory of variational hybrid quantum-classical algorithms, New Journal of Physics 18 (2) (2016) 023023.

[28] M. O. S. N. Wolberg, William, W. Street, Breast Cancer Wisconsin (Diagnostic), UCI Machine Learning Repository, DOI: https://doi.org/10.24432/C5DW2B (1993).

[29] V. Lohweg, Banknote Authentication, UCI Machine Learning Repository, DOI: https://doi.org/10.24432/C55P57 (2012).

[30] F. Fontanella, DARWIN, UCI Machine Learning Repository, DOI: https://doi.org/10.24432/C55D0K (2022).

[31] K. Pearson, On the criterion that a given system of deviations from the probable in the case of a correlated system of variables is such that it can be reasonably supposed to have arisen from random sampling, Philosophical Magazine Series 5 50 (302) (1900) 157–175.

[32] Y. LeCun, Y. Bengio, G. Hinton, Deep learning, Nature 521 (7553) (2015) 436–444.

[33] M. A. Nielsen, I. L. Chuang, Quantum Computation and Quantum Information, Cambridge University Press, 2010.

[34] P. Wittek, Quantum Machine Learning: What Quantum Computing Means to Data Mining, Academic Press, 2014.

[35] J. Preskill, Quantum computing in the nisq era and beyond, Quantum 2 (2018) 79.

[36] F. Arute, K. Arya, R. Babbush, et al., Quantum supremacy using a programmable superconducting processor, Nature 574 (7779) (2019) 505–510.

[37] G. Research, Quantum machine learning and the power of data, accessed: 2025-01-12 (2022).
URL https://research.google/blog/quantum-machine-learning-and-the-power-of-data/

[38] M. Rath, H. Date, Quantum data encoding: A comparative analysis of classical-to-quantum mapping techniques and their impact on machine learning accuracy (2023). arXiv:2311.10375.
URL https://arxiv.org/abs/2311.10375

[39] Y. Zhang, Q. Ni, Recent advances in quantum machine learning, Quantum Engineering 2 (1) (2020) e34.

[40] I. Jolliffe, Principal Component Analysis, Springer, 2002.

[41] B. Schölkopf, A. Smola, K.-R. Müller, Nonlinear component analysis as a kernel eigenvalue problem, Neural Computation 10 (5) (1998) 1299–1319. doi:10.1162/089976698300017467.

[42] C. M. Bishop, Pattern Recognition and Machine Learning, Springer, 2006.

[43] M. A. Nielsen, I. L. Chuang, Quantum Computation and Quantum Information, Cambridge University Press, 2002.

[44] J. Preskill, Quantum computing in the nisq era and beyond, Quantum 2 (2018) 79.

[45] S. Lloyd, M. Mohseni, P. Rebentrost, Quantum principal component analysis, Nature Physics 10 (2014) 631–633.

[46] S. L. Aram W. Harrow, Avinatan Hassidim, Quantum algorithms for linear systems of equations, Physical Review Letters 103 (2009) 150502.

[47] P. Shor, Polynomial-time algorithms for prime factorization and discrete logarithms on a quantum computer, SIAM Journal on Computing 26 (1999) 1484–1509.

[48] M. Schuld, F. Petruccione, Quantum Machine Learning: An Introduction, Springer, 2019.

[49] E. Dri, A. Aita, T. Fioravanti, G. Franco, E. Giusto, G. Ranieri, D. Corbelletto, B. Montrucchio, Towards an end-to-end approach for quantum principal component analysis, 2023 IEEE International Conference on Quantum Computing and Engineering (QCE) 02 (2023) 1–6.
URL `https://api.semanticscholar.org/CorpusID:265526097`

[50] D. P. Kingma, M. Welling, Auto-encoding variational bayes, arXiv preprint arXiv:1312.6114 (2013).

[51] J. Romero, J. P. Olson, A. Aspuru-Guzik, Quantum generative adversarial learning, Quantum Science and Technology 2 (4) (2017) 045001.

[52] M. Benedetti, E. Lloyd, S. Sack, M. Fiorentini, Parameterized quantum circuits as machine learning models, Quantum Science and Technology 4 (4) (2019) 043001.

[53] C. Cortes, V. Vapnik, Support-vector networks, Machine Learning 20 (3) (1995) 273–297.

[54] N. Cristianini, J. Shawe-Taylor, An Introduction to Support Vector Machines and Other Kernel-based Learning Methods, Cambridge University Press, New York, NY, USA, 2000.

[55] M. Altaisky, N. Kaputkina, V. Krylov, Quantum neural networks: Current status and prospects for development, Physics of Particles and Nuclei 45 (2014) 1013–1032.

[56] F. Tacchino, C. Macchiavello, D. Gerace, D. Bajoni, An artificial neuron implemented on an actual quantum processor, npj Quantum Information 5 (1) (2019) 26.

[57] X. Niu, W. Ma, A novel quantum neural network based on multi-level activation function, Laser Physics Letters 18 (2) (2021) 025201.